General Disclaimer

One or more of the Following Statements may affect this Document

- This document has been reproduced from the best copy furnished by the organizational source. It is being released in the interest of making available as much information as possible.

- This document may contain data, which exceeds the sheet parameters. It was furnished in this condition by the organizational source and is the best copy available.

- This document may contain tone-on-tone or color graphs, charts and/or pictures, which have been reproduced in black and white.

- This document is paginated as submitted by the original source.

- Portions of this document are not fully legible due to the historical nature of some of the material. However, it is the best reproduction available from the original submission.

STRUCTURE OF IMPULSIVE PHASE OF SOLAR FLARES FROM MICROWAVE OBSERVATIONS

by

Vahé Petrosian

July 1981

SUIPR No. 847

National Aeronautics and Space Administration

Grants NSG 7092 and ~~NGL 272~~ NGL-05-020-272

Institute for Plasma Research
Stanford University
Stanford, California

STRUCTURE OF IMPULSIVE PHASE OF SOLAR FLARES FROM MICROWAVE OBSERVATIONS

Vahé Petrosian[1]

Institute for Plasma Research

Stanford University

Stanford, CA

[1]Also Department of Applied Physics

ABSTRACT

Variation of the microwave intensity and spectrum due to gyro-synchrotron radiation from semi-relativistic particles injected at the top of a closed magnetic loop has been described. Using the recent high spatial resolution x-ray observations from the HXIS experiment of the SMM and from observations by the VLA, it is shown that the high microwave brightness observed at the top of the flare loop can come about if i) the magnetic field from top to footpoints of the loop does not increase very rapidly, and ii) the accelerated particles injected in the loop have a nearly isotropic pitch angle distribution. The limits on the rate of increase of the magnetic field and/or the average pitch angle depend on the geometry and location of the loop on the solar disk.

I. INTRODUCTION

Close correlation between the observed temporal variation of the hard x-rays and microwave radiation during the impulsive phase of solar flares indicates that the same (or a closely related) population of electrons are responsible for both of these radiations. It is assumed that a wide energy spectrum of electrons is produced during the impulsive phase, with the lower energy ones ($\varepsilon \lesssim 100$ keV) being responsible for the bulk of the observed hard x-rays and the higher energy ones ($\varepsilon \gtrsim$ few hundred keV) producing the microwave radiation. However, one of puzzling results obtained from the SMM HXIS experiment and the high resolution ground-base microwave observations has been that the x-rays (15 to 30 keV) and the microwave radiation (at wavelengths of 2 to 6 cm) are not coming from the same region. In the few events observed, the tendency is for the bulk of x-rays to come from the foot points of flare loops (Hoyng et al 1981) while the microwaves are observed to come primarily from the top of the loop (Marsh and Hurford 1980; Marsh et al 1980; Kundu et al 1981).

The purpose of this letter is to investigate the limitation that these observations impose on the parameters of proposed models of flares.

In general, x-rays which are produced by bremsstrahlung are simpler to analyze and give more direct information about the characteristics of the accelerated electrons. In almost all models the x-ray intensity is expected to increase from top to the foot points of the loop because of higher densities at lower regions (see Emslie 1981).

On the other hand, the microwave radiation, produced by gyro-synchrotron process, depends on the pitch angle distribution of the electrons, on the magnetic field structure and is affected by various absorption processes (Ramaty and Petrosian 1972). In two recent works we have developed a simple description of the variation along a magnetic loop of the pitch angle and energy distribu-

tion of electrons injected at the top of the loop (Leach and Petrosian 1981, hereafter referred to as LPI) and have derived simple analytic formulas for evaluation of the gyro-synchrotron flux from semi-relativistic particles with arbitrary pitch angle and energy distributions (Petrosian 1981, PI). We use these results to evaluate the variation of the microwave flux along a single flaring loop and compare it with observations. In this letter we consider the general features of the models. A more detailed analysis will be published elsewhere.

II. GENERAL DESCRIPTION

To simplify our analysis we consider a flaring loop of width D, length πR and a central magnetic field line which is a semicircle (see Figure 1a). We assume that the strength of the magnetic field B increases from top to the footpoints (symmetrically), $B = B_0 b(s)$, so that the width also varies as $D^2 = D_0^2/b$. This means that other (non-central) field lines will deviate from the assumed circular configuration but if $D \ll ds/d\ln B$, such deviations can be ignored. If the distribution $f_s(\mu,\gamma)$ in pitch angle cosine μ and energy γ of electrons along the loop is known ($fd\mu d\gamma ds$ is the number density of electrons within μ to $\mu + d\mu$, γ to $\gamma + d\gamma$ and s to $s + ds$), then the gyro-synchrotron emissivity $j_\nu(s,\theta)$ at frequency ν and in the direction θ with respect to the field lines can be calculated using the equations in PI;

$$j_\nu(s,\theta) = (e^2\nu_b \sin\theta/c)(\nu/\nu_b \sin\theta)^{\frac{1}{2}} f_s(\beta_o \cos\theta, \gamma_o)\, G(\theta,\gamma_o) \ . \qquad (1)$$

Here, $G(\theta,\gamma_o)$ is a slowly varying function of θ and, in general, like f_s, decreases with increasing γ_o, $\nu_b = eB/2\pi mc = 2.8 \times 10^6$ Hz(B/gauss) is the gyro-frequency and γ_o (the energy of the electrons with the highest contribution to the emissivity, $\beta_o^2 = 1 - \gamma_o^{-2}$) depends on the energy spectrum of the electrons. For electrons with pitch angle distributions which are not extremely anisotropic and have a power law energy spectrum, $f_s(\mu,\gamma) \propto (\varepsilon_c - 1 + \gamma)^{-\delta}$, or for a thermal electron gas with temperature kT (in units of mc^2), $f(\mu,\gamma) \propto \gamma(\gamma^2-1)^{\frac{1}{2}} e^{-(\gamma-1)/kT}$ and to a good approximation (cf. PI);

$$(\gamma_o^2 - 1) = \begin{cases} 4\nu/[3\nu_b(\delta+1)\sin\theta], & \varepsilon_c \approx 1 \\ (2\nu kT/\nu_b)(1 + 4.5\nu kT \sin^2\theta/\nu_b)^{-1/3}, & kT \lesssim 1 \end{cases} \ . \qquad (2)$$

In the optically thin regime, $\nu > \nu^*$, the observed intensity is

$$I_\nu(s,\theta) \simeq \int j_\nu(s,\theta)dl \simeq j_\nu(s,\theta)D_o/b^{\frac{1}{2}}\sin\theta, \quad \nu > \nu^* \tag{3}$$

As frequency decreases, I_ν rises till the critical frequency ν^*, where the optical depth is of order unity; then with further decrease in ν (optically thick regime), it begins to decrease. As mentioned above, it is not clear which absorption mechanism will be the dominant one. Except for self-absorption the other mechanisms depend on the ambient plasma parameters. Because of model dependence of these other absorption processes, we will consider only the self-absorption process, in which case the intensity can be approximated by

$$I_\nu \simeq 2\langle E\rangle m\nu^2, \quad \text{for} \quad \nu < \nu^* . \tag{4}$$

Here $\langle E\rangle$ is some average particle kinetic energy (in units of mc^2, $E = \gamma - 1$). For a Maxwellian distribution $\langle E\rangle = kT$ and $I_\nu \propto \nu^2$. For a power law distribution, at $\nu \gg \nu_b$, $\langle E\rangle \simeq \gamma_o - 1 \cong \nu^{\frac{1}{2}}$ so that $I_\nu \propto \nu^{5/2}$. The critical frequency ν^* is a complicated function of ν_b, θ and D; $\nu^* = \nu_b \sin\theta\, H(\nu_b,\theta,D)$. However, in most cases H is a slowly varying function of the parameters. We will ignore its variation and set $\nu^* = H_o\nu_b\sin\theta$.

As is evident from eqs. (1) to (4), the spectrum and flux of the gyro-synchrotron radiation depends primarily on the particle distribution function f. Thus, before we can calculate the emissivity we need to specify the variation of density, pitch angle distribution and energy spectrum of the electrons along the field lines. This is the most complex part of the problem and the part which depends strongly on the assumptions of the models, on the many unknowns

of the flare plasma and the acceleration of the particles. Below we shall consider a few forms for this distribution covering most of the proposed models for the impulsive phase of solar flares.

III. SOME MODELS

The characteristics of the models depend on the distribution in phase space of the accelerated particles and on the variation of the magnetic field and plasma density along the loop.

These properties depend on the combination of average pitch angle α_o, the quantity $R d\ln B/ds$ and on the dimensionless column depth $d\tau_E = [4\pi r_o^2 \ln\Lambda (E+1)/E^2] n ds$ (n is the ambient electron density, $r_o = 2.8 \times 10^{-13}$cm and $\ln\Lambda \approx 20$). For example, if the electrons, injected at the top of the loop, have small pitch angles ($\alpha_o \ll 1$) and the magnetic field is nearly uniform ($R d\ln B/ds \ll 1$) a beamed thick target model will be the result. The x-rays of energy E then will be produced primarily at the regions where the column depth τ_E, measured from the top of the loop, is of order unity. This is because the number of electrons with kinetic energy E decreases rapidly when τ_E exceeds unity (cf. figures 3 and 7 of LPI). The HXIS observation that the 20 keV x-rays originate primarily from the footpoints indicates that $\tau_{.04} \lesssim 1$ throughout most of the loop, which means electrons are injected at a column depth $N = \int n ds \lesssim 10^{20} \mathrm{cm}^{-2}$ above the footpoint (or the transition region). Note that for high energy electrons needed for the microwave radiation this means $\tau_{E>1} < 0.001$.

In the other extreme case, if particle distribution is nearly isotropic (α_o of order unity) and the magnetic field varies rapidly ($R d\ln B/ds \gg 1$ for $\tau_E \ll 1$), then the electrons will be trapped and radiate x-rays primarily from regions with the highest magnetic field and ambient density which again will be the lower parts of the loop. In general, the parameter which determines the degree of beaming or trapping is

$$\zeta_E \equiv \sin^2\alpha_o \left\langle d\ln B/d\tau_E \right\rangle . \qquad (5)$$

For $\zeta_E << 1$ one has a beamed model and for $\zeta_E >> 1$ a trapped model. In the low density regions of the loop ($\tau_E << 1$), $\zeta_E >> 1$ and the distribution of particles are determined by the adiabatic invariance of $B/\sin^2\alpha$. For example, for an injected spectrum at $\tau = 0$ of $f_0(\sin^2\alpha,E)$, the distribution along the loop becomes (cf. LPI, eq. 7)

$$f_s(\sin^2\alpha,E) = f_0(\sin^2\alpha/b,E) \tag{6}$$

On the other hand, if the density is large so that τ_E exceeds unity much before the magnetic field has changed significantly, then the particle distribution is determined by the collisions with the ambient plasma. In general, there is no simple analytic expression for the distribution except in the small pitch angle regime. For example, for injected electrons with gaussian pitch angle distribution and energy spectrum $f_0(E)$, eq. (18) of LPI for relativistic energies gives

$$f_s(\mu,E) = f_0(E\zeta)\ 2\alpha\exp\left[-\frac{\alpha^2}{\alpha_0^2+\ln\zeta}\right]\Big/(\alpha_0^2+\ln\zeta),\quad \zeta = 1+\tau_E\ . \tag{7}$$

For non-relativistic energies $f_0(E\zeta) \to f_0(E\zeta^{\frac{1}{2}})/\zeta^{\frac{1}{2}}$.

We now consider the microwave radiation from a few models with different values of the parameter ζ_E.

1) Uniform Trap Model. Let us first consider the simplest (but somewhat unrealistic) model with nearly uniform magnetic field and isotropic pitch angle distribution. Such a model will result if $\tau_E << 1$ and if particles are injected isotropically at the top, so that according to equation (6) $f_s(\mu,E) = f_0(E)$. Of course, to have a trap model, the magnetic field

must eventually vary. We assume $B = \text{const}$ throughout except at the footpoints where $B \to \infty$ rapidly.

Since the magnetic field is uniform ($\nu_b = \text{const}$), then, according to our earlier discussion, ν^* and $(\gamma_o^2 - 1)^{-1}$ will vary as $\sin\theta$ so that the spectrum and intensity of the microwave radiation will depend primarily on $\sin\theta$ and the frequency of observation. In Figure 2a we show schematically the variation of ν^*, γ_o and $f_s(\gamma_o)G$ with $\cos\theta$ at a given frequency. At higher (lower) frequencies, the γ_o curve is shifted to higher (lower) values. The quantity $f_s(\gamma_o)G$ then changes accordingly, decreasing the increasing γ_o. In Figures 2b and 2c we show the expected microwave spectra at a few values of θ ($\theta = \pi/2$ for the highest curve). For power law spectra, the spectra cross each other because in the optically thick region $I_\nu \propto \gamma_o - 1$, while for a thermal source of uniform temperature, $I_\nu \propto kT$.

As evident from these figures the variation of intensity with θ will depend on the frequency. As shown in Figure 2d, at $\nu > \nu^*_{max}$, the maximum turnover frequency, the optical depth $\tau_\nu << 1$ for all θ so that $I_\nu \propto f \times G$ (cf. eqs 1 and 3) decreases rapidly. For $\nu < \nu^*_{max}$ the intensity increases slowly (as γ_o-1, for power law) or remains constant (thermal) for $|\cos\theta| < \cos\theta_{crit}$ where $\nu^*(\theta_{crit}) = \nu$ and $\tau_\nu = 1$. For $\cos\theta > \cos\theta_{crit}$ $\tau_\nu < 1$ and the intensity decreases rapidly again as $f \times G$.

The angle θ and consequently the variation of the intensity along the loop depends on the angle $\eta = s/R$ (cf. Figure 1a) and on the location and orientation of the loop on the sun. In general, for a loop near the solar equator, at heliocentric longitude ϕ

$$\pm\cos\theta = \cos\phi\sin\eta + \cos\psi\sin\phi\cos\eta \quad , \tag{8}$$

where ψ is the angle between the projection of the loop and the solar equator (see Fig. 1b). In general, the location along the loop (i.e., the value of η) where the intensity is maximum ($\cos\theta = 0$) will vary with ϕ and ψ.

For a loop near the center of the solar disk ($\phi \approx 0$ and all ψ) $\cos\theta = \pm\sin\eta$ so that the intensity will be highest at the top of the loop. As we move away from the center $\phi > 0$, the maximum intensity ($\theta = \pi/2$) occurs at $\eta_{max} \neq 0$ (e.g. $\eta = \phi$ for $\psi = 0$). However, when projected on the solar disk the maximum intensity will appear approximately half way betweeen the footpoints[1].

[1]Note that for $\phi \neq 0$ the microwave emission will not necessarily be symmetric. This kind of configuration rather than an asymmetric field geometry, may be the explanation of some observed asymmetries (Alissandrakis and Kundu 1978; Kundu and Vlahos 1979).

This picture will change near the limb ($\phi = \pi/2$) where for $\psi = \pi/2$, $\theta = \pi/2$ and the microwave intensity is uniform all along the loop or for $\psi = 0$, $\cos\theta = \cos\eta$ and the highest intensity occurs at the footpoints. However, the observations under consideration here with two distinct footpoints do not refer to these configurations.

We conclude, therefore, that this model agrees with the microwave observations. The basic reason is that it is the value of the component of the magnetic field perpendicular to the line of sight which determines the brightness of a synchrotron source. Furthermore, as shown in Figure 2d, the variation of the intensity (along the loop) is strongest at the highest frequency, so that the source of the microwave radiation will appear smaller (more concentrated toward the middle of the footpoints) at higher frequencies. Comparison of the 2 cm (Marsh and Hurford 1980) observations and at 6 cm (Kundu et al 1981) agrees with this aspect of the model.

The flux from the whole loop can be obtained by integration of the intensity along the loop. As shown by the dashed line in Figure 2b or 2c at $\nu > \nu^*_{max}$ the total flux will be decreasing as in eq. (3) with most of the contribution

coming from $\theta = \pi/2$. At lower frequencies the contribution from other parts begin to become significant, and the total spectrum will be somewhat flatter than (but will approach asympthotically to) the spectrum in eq. (4). This type of spectrum is commonly observed (Hurford, Marsh and Zirin 1981; see also Solar Geophysical Data) and is attributed to inhomogeneities in the source or to other absorption processes (Ramaty and Petrosian 1972). We can see here that even a uniform loop (uniform in field strength and particle distribution) can qualitatively reproduce such observed microwave spectra.

Note that the above picture remains qualitatively the same even for non-uniform magnetic field as long as the magnetic field variation is slower than $1/\sin\theta$. Any such variation, however, would give rise to a slower variation of the intensity along the loop and to stronger asymmetries for loops away from the center of the disk.

2) Non-uniform Trap Model ($\zeta_E \gg 1$). Now we consider a model where the magnetic field varies rapidly throughout the loop ($R d\ln B/ds \gg 1$) instead of the extreme variation concentrated at the footpoints of the above model. As mentioned above, particles responsible for the microwave emission have $\tau_E \ll 1$ so that for α_o of order unity $\zeta_E \gg 1$. As in model (1) the pitch angle distribution is governed by eq. (6), according to which the distribution broadens as the field strength increases.

This model is different from model (1) not only in its allowance for non-isotropic distribution but, more importantly, because of its rapid variation of the magnetic field (and ν_b), both ν^* and γ_o^{-1} increase from top to lower parts of the loop reversing the trends of model (1). The dashed line on Figure 2a shows the schematic variation of ν^* (the decrease near $\cos\theta = \pm 1$ is due to the unrealistic circular shape of the assumed loop). This increase in ν^* (and the decrease in γ_o and the increase in $f \times G$) is stronger for loops

away from the center of the disk. In this model then the top curves on Figures 2b and 2c will correspond to the footpoints of the loop such that the trend in Figure 2d is reversed, as shown by the dashed line which clearly disagrees with observations.

3) Uniform Beamed Model ($\zeta_E << 1$). Now we complicate the models by injecting electrons non-isotropically with small pitch angles. If the magnetic field is constant or varies slowly, then $\zeta_E << 1$. The variation of ν^* and γ_o in this model will be similar to that of model (1). However, the quantity $f(\beta_o \cos\theta, \gamma_o)G$ will now vary not only because of variation of γ_o but also because of the non-isotropic nature of the distribution and the variation of $\beta_o \cos\theta$ along the loop. For this model the variation of the distribution is given by eq. (7). As mentioned above, along most of the loop $\tau_{E>1} < 10^{-3}$ so that if α_o is greater than a few degrees, then in eq. (7) $\ln\zeta < \alpha_o^2$, $\alpha = \cos^{-1}(\beta_o \cos\theta) \approx \theta$ and $f_s(\beta_o \cos\theta, E_o) \propto f_o(E_o) \exp(-\theta^2/\alpha_o^2)$.

For all orientations and locations of the loop we have at the footpoints $\pi/2 < \theta < \pi$ and at the top $0 < \theta < \pi/2$ so that the value of f is, in general, much larger at the top, which makes the variation of $I_\nu(\theta)$ in Figure 2d even steeper than that of model 1. There are, however, two problems with this result. First of all, the stronger the beaming the fewer the number of particles contributing to the flux. If the self-absorption was not important, this would be a natural explanation of the old discrepancy between the number of electrons needed for x-ray and microwave emission. However, with strong self-absorption this model will produce less microwave flux than observed. The second difficulty with this model is that eq. (7) is valid for small pitch angles while we are interested in values of f, typically, at $\alpha \simeq \pi/2$. As inspection of Figure 1 of LPI will show, the number of particles at such large pitch angles can vary by large factors with slight changes in the value of α_o, α

or in the field geometry. Thus, it is difficult to make a definite statement about the validity of this model.

4) Non-uniform Beamed Model ($\zeta_E >> 1$). Finally, we consider a model diametrically opposite of model 1 in that the field varies strongly and particle pitch angle distribution is non-isotropic. Since the magnetic field varies strongly, we have a situation similar to model 2 where ν^* increases with $\cos\theta$ (see dashed line in Figure 2a) and γ_o decreases with $\cos\theta$. Here, $f(\beta_o\cos\theta,\gamma_o)$ increases with $\cos\theta$ not only because of the decrease of γ_o (as in model 2) but also because of variation of $\beta_o\cos\theta$. As evident from eq. (6), the pitch distribution broadens with increasing field strength, giving rise to a larger value of $f(\beta_o\cos\theta,\gamma_o)$ at the footpoints as compared to the top. For example, for a gaussian injected spectrum in a loop at the center of the disk $f_{\eta=0}(\beta_o\cos\theta,\gamma_o) \propto \exp(-\alpha_o^{-2}) << 1$ at the top of the loop, while at the footpoints where $\beta_o\cos\theta = -1$ and $b >> 1$, $f_{\eta=\pi/2}$ is about unity. Thus, in contradiction with observations, $I_\nu(\theta)$ varies even faster than that given by the dashed line in Figure 2d.

IV. SUMMARY

We have presented a qualitative description of microwave emission from electrons injected at the top of a closed loop with particular attention to the variation of intensity and spectrum along the loop. As evident from the discussion of previous sections, many parameters enter into this description of the models. We emphasize here the effects of the orientation, location and geometry of the loops and the pitch angle distribution of the accelerated electrons.

We have considered the total intensity (disregarding the polarization) for four models which qualitatively agree with the HXIS observation of $\sim$20 keV x-rays. We find that the high resolution microwave observations can be reproduced by models where the magnetic field increases slowly from the top of the loop to its footpoints at the transition region. Faster field variations give stronger emission at the footpoints. In addition, another requirement is that the accelerated particle distribution should be nearly isotropic. Model 1 satisfies both these requirements. If the accelerated particles are strongly beamed along the field lines, then the footpoints will be brighter than the top for a rapidly increasing magnetic field, but for a uniform field the situation is uncertain and a more detailed analysis of the pitch angle distribution is needed.

We have considered models with the extreme value of the critical parameter ζ_E. For intermediate values of this parameter results intermediate to those described will be obtained.

We have neglected absorption process other than the self-absorption. These other processes will be more important at the lower, high density, regions of of the loop and, therefore, could reduce the intensity of the footpoints

(see e.g. Ramaty 1969, for effects of Razin-Tsytovich suppression mechanism). These and consequences of our other simplifying assumptions, in particular, setting $\nu^* = H_o \nu_b \sin\theta$, along with the expected variation of the polarization, will be described elsewhere.

ACKNOWLEDGMENT

I would like to thank Dr. Gordon Emslie for his many valuable comments and discussions.

This work was supported by the National Aeronautics and Space Administration under Grants NSG 7092 and NGL 272.

REFERENCES

Alissandrakis, C.E. and Kundu, M.R. 1978, Ap. J., 222, 342.

Emslie, A.G. 1981, Ap. J., 245, 711.

Hoyng, P., Duijveman, A., Machado, M.E., Rust, D.M., Svestka, A., Boelee, A., de Jager, C., Frost, K.J., Lafleur, H., Simnett, G.M., van Beek, H.F. and Woodgate, B.E. 1981, Ap. J. (Letters), 246, L155.

Hurford, G.J., Marsh, K.A. and Zirin, H. 1981, AAS Bulletin 13, 553.

Kundu, M.R., Bobrowsky, M. and Velusamy, T. 1981, (Preprint, in press).

Kundu, M.R. and Vlahos, L. 1979, Ap. J. 232, 595.

Leach, J. and Petrosian, V. 1981, Ap. J., 250, (in press).

Marsh, K.A. and Hurford, G.J. 1980, Ap. J. (Letters), 240, L111.

Marsh, K.A., Hurford, G.J., Zirin, H. and Hjellming, R.M. 1980, Ap. J., 242, 352.

Petrosian, V. 1981, Ap. J., 250, (in press).

Ramaty, R. 1969, Ap. J., 158, 753.

FIGURE CAPTIONS

Figure 1. Geometry of loops on the sun.

a) Assumed geometry for a loop. Electrons are injected at the top $\eta = \frac{S}{R} = 0$, $\tau_E = 0$. The indicated values of $\cos\theta$ is for a loop at the center of the disk.

b) Loops at various solar longitude ϕ and orientation ψ. For loops at the center of disk $\cos\theta = \pm\sin\eta$, at the limb $\theta = \pi/2$ throughout if $\psi = \pi/2$ and $\cos\theta = \cos\eta$ if $\psi = 0$. Note that for loops with distinct footpoints the point where line of sight is perpendicular to the field line will appear midway between the footpoints.

Figure 2. Schematic representations of variation of various quantities with angle θ and frequency ν for model 1.

a) Variation of the critical frequency ν^*, energy γ_o and $Gf(\gamma_o)$, the quantity determining the emissivity in the optically thin region, with $\cos\theta$ (dashed line for model 2).

b) Synchrotron spectra at different values of θ for a power law electron spectrum. $|\cos\theta| = 0$ ($\theta = \pi/2$) for the curve with $\nu^* = \nu^*_{max}$ and increase gradually for the lower curves. Dashed line for the spectrum integrated over all angles θ.

c) Same as (b) except for a Maxwellian electron distribution.

d) Variation of intensity with $\cos\theta$ at two different frequencies (dashed line for model 2). The location of the top and footpoints are shown for a loop at the center of the solar disk. For loops with $\psi = \pi/2$ the footpoints move in the direction of the arrow as the loop moves from the center to the limb. At the limb all points along the loop are at $\cos\theta = 0$.

Vahe Petrosian

Institute for Plasma Research

Stanford University

Stanford, CA 94305

(415) 497-1435

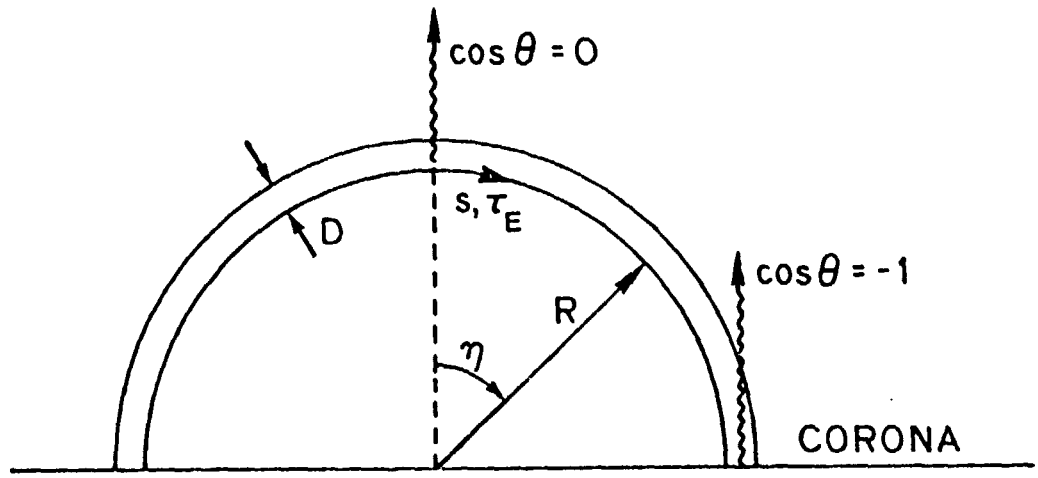

(a) A LOOP

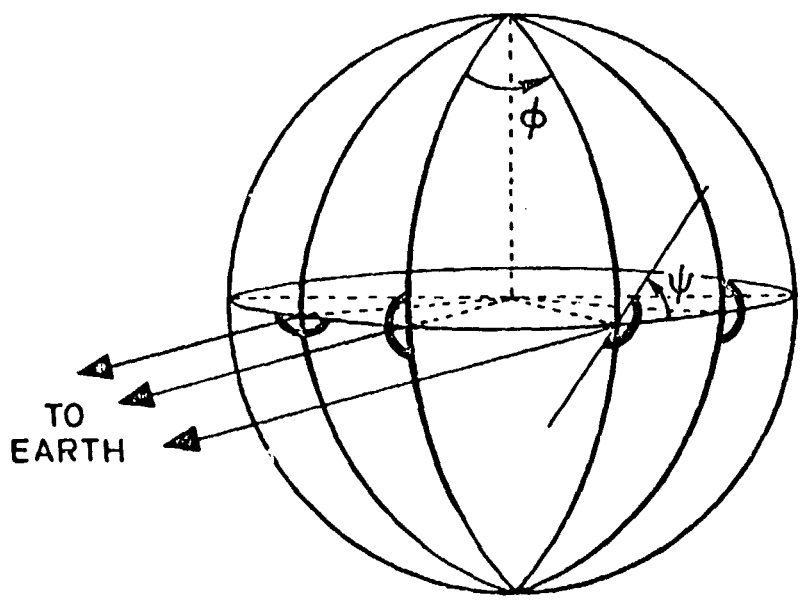

(b) LOOPS ON THE SUN

Figure 1

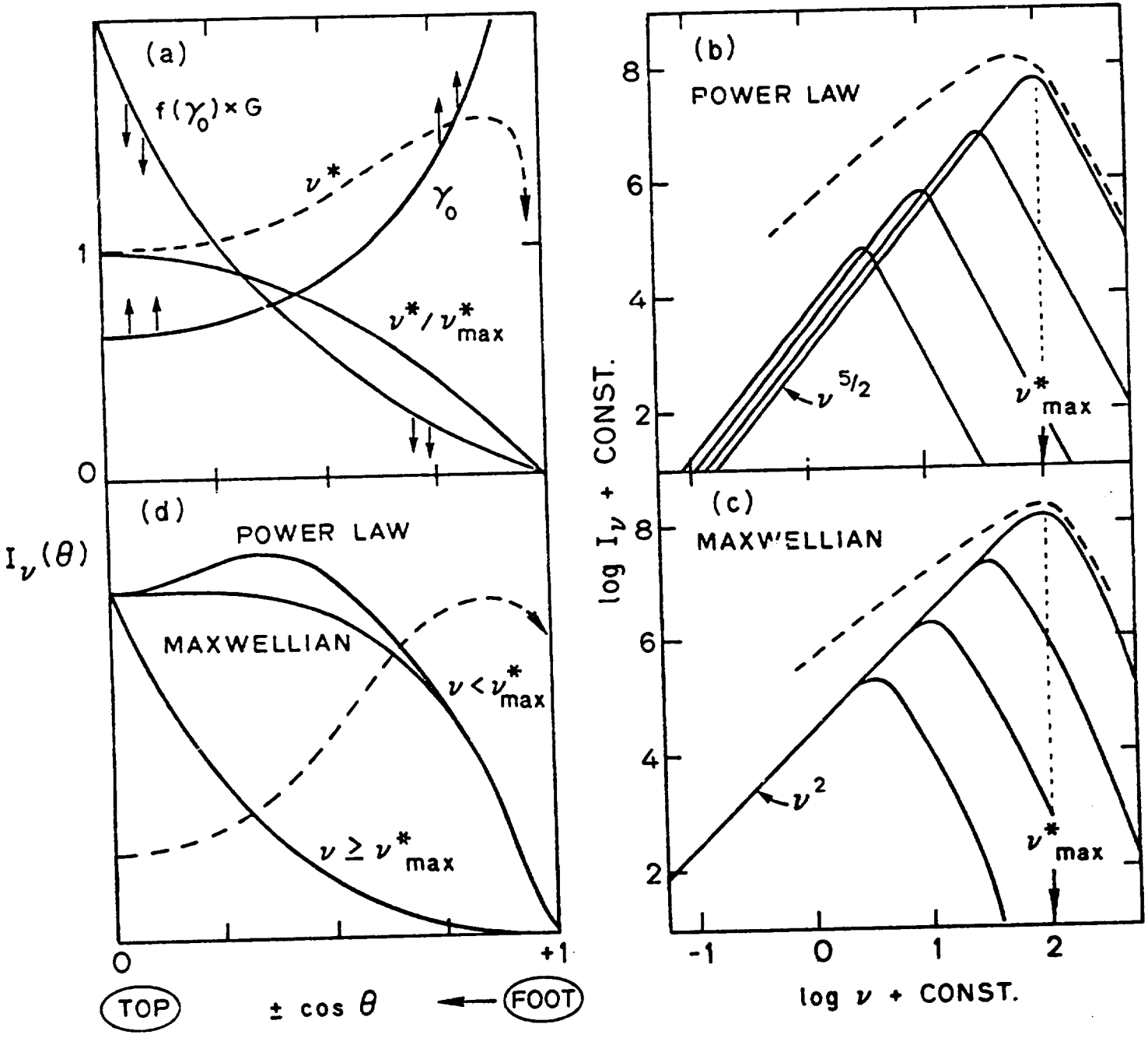
(a)
f(γ0)×G
ν*
γ0
1
ν*/ν*max
0
(b)
POWER LAW
8
6
4
2
ν 5/2
ν*max
(d)
POWER LAW
Iν(θ)
MAXWELLIAN
ν<ν*max
ν≥ν*max
0
+1
TOP
± cos θ
FOOT
(c)
MAXWELLIAN
log Iν + CONST.
8
6
4
2
ν2
ν*max
-1
0
1
2
log ν + CONST.